Chapter 34
Detection of Gas Raman Spectra Based on Double-Cladding Fiber Laser

Chun Feng and Shu-Bo Jiang

Abstract To improve the Raman scattering cross-section of trace gases, a Raman spectrum detection method based on the double-clad fiber laser is designed in this paper. The influence of double-cladding fiber laser as a light source on gas Raman detection is investigated. The higher the output power of the double-clad fiber laser, the larger the gas scattering cross-section and the stronger the Raman effect. Therefore, this paper first conducts a numerical analysis of the factors affecting the output power of the double-clad fiber laser and uses MATLAB to simulate and explore the influence of different pumping modes, pumping power, and rare earth doping concentration on the output power of the fiber laser. Then the gas detection system with ytterbium-doped fiber laser as the light source was used to analyze the material qualitatively and quantitatively. Fiber laser as a Raman detection source has the advantages of high linearity and good stability.

34.1 Introduction

Raman spectrum is a kind of scattering spectrum, which can obtain the information of molecular vibration and rotation through the analysis of the scattering spectrum different from the incident light frequency, and is applied to the study of molecular structure [1]. It can realize the qualitative and quantitative analysis of substances. At the same time, it is a non-contact detection method that can carry on the nondestructive detection to the material. However, Raman scattering is a weak effect. With the development of laser technology, the incident light intensity is improved. The Raman effect is enhanced and the application of Raman spectroscopy is promoted. Therefore, the laser can be used as the Raman detection light source [2].

Since the birth of the first laser, a series of lasers, such as solid-state laser, gas laser, and semiconductor laser, have been developed rapidly. The optical fiber laser instrument has been widely used in optical communication, spectroscopy, aerospace, and

C. Feng · S.-B. Jiang (✉)
College of Electrical Engineering and Control Science, NanJing Tech University, NanJing 211816, China
e-mail: jiangshubo@njtech.edu.cn

G. Liu and F. Cen (eds.), *Advances in Precision Instruments and Optical Engineering*, Springer Proceedings in Physics 270, https://doi.org/10.1007/978-981-16-7258-3_34

laser weapons because of its good beam quality, high conversion efficiency, convenient thermal control and management, large tunable range, and compact structure [3, 4]. In order to further improve the conversion efficiency and output power of conventional fiber laser, double-clad fiber lasers began to appear. It is a kind of optical fiber with a special structure; it has an inner cladding than the conventional optical fiber. The transverse size and numerical aperture of the inner cladding are far larger than that of the fiber core. When rare earth elements are doped in the core, the pump light is reflected in the inner cladding and is absorbed by the doped ions through the core many times, thus being converted into a single-mode laser efficiently. The conversion efficiency of traditional fiber lasers is greatly improved [5].

Based on the principle of double-clad fiber laser, this paper analyzes the fiber laser as a Raman detection source, selects high-power diode-pumped laser, ytterbium-doped double-clad fiber, adopts forward pumping mode and traditional detection optical path, and sets up an oxygen-based Raman gas detection system.

34.2 Basic Theory and Simulation of Double-Clad Fiber Laser

34.2.1 Theoretical Model of Double-Clad Fiber Laser

The theoretical model construction of fiber laser is shown in Fig. 34.1. The fiber laser is composed of fiber combiner, fiber grating, pump source, and double-cladding gain fiber. Instead of discrete optical devices, the optical fiber combiner can effectively make the pump light coupling into the double-clad fiber, reduce the loss and improve the coupling efficiency. At the same time, the output of multiple semiconductor lasers can be connected at the input end of the double-clad fiber to improve the injectable pump power. Fiber Bragg grating FBG1 and FBG2 can be used to achieve fixed wavelength reflection and absorption. The pump source uses semiconductor diodes, double-clad optical fibers [6], and is several meters to dozens of meters in length. The pump light is coupled to the optical fiber through the optical fiber combiner, and the doped rare earth ions in the optical fiber absorb the pump energy, and the energy-level transition occurs, which makes the particles accumulate continuously and form the particle inversion [7]. Then the transition to the lower energy level of the laser produces photons, which are oscillated and amplified in the resonator and

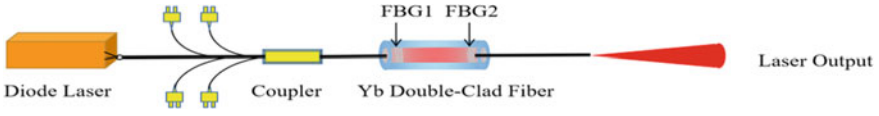

Fig. 34.1 Theoretical model of fiber laser

form the laser output from the grating. The formation of the laser is related to its rate equation. Next, the rate equation of fiber laser is analyzed.

34.2.2 Rate Equation of Double-Clad Fiber Laser

The laser rate equation is used to characterize the differential equations of the number of atoms at each energy level and the number of photons in the cavity changing with time. It is used to describe the interaction between the radiation field and particles. When only pumping light and laser output line width are considered, the rate equations of double-clad fiber lasers can be simplified as follows [7]:

$$\begin{cases} \frac{dP_P^+(z)}{dz} = -\Gamma_P[\sigma_{ap}N - (\sigma_{ap}+\sigma_{ep})N_2(z)]P_p^+(z) - a_p P_P^+(z) \\ \frac{dP_P^-(z)}{dz} = -\Gamma_P[\sigma_{ap}N - (\sigma_{ap}+\sigma_{ep})N_2(z)]P_p^-(z) + a_p P_P^-(z) \\ \frac{dP_s^+(z)}{dz} = -\Gamma_s[(\sigma_{es}+\sigma_{as})N_2(z) - \sigma_{as}]P_s^+(z) - \Gamma_s\sigma_{es}N_2(z)P_0 - a_s P_s^-(z) \\ \frac{dP_s^-(z)}{dz} = -\Gamma_s[(\sigma_{es}+\sigma_{as})N_2(z) - \sigma_{as}]P_s^-(z) - \Gamma_s\sigma_{es}N_2(z)P_0 - a_s P_s^-(z) \end{cases} \tag{34.1}$$

Formula 34.1 describes the relationship between the concentration of upper-level particles in the gain medium at different positions and the pumping power of the forward and backward light, where $N_2(z)$ is the concentration of particles at the upper level. $P_P^+(z)$ and $P_p^-(z)$ are, respectively, the power of pumping light forward and backward; $P_s^+(z)$ and $P_s^-(z)$ refer to the forward and backward transmission power, where N is the concentration of doping medium in the fiber core, A_c is the cross-sectional area of the fiber core, and Γ_P and Γ_s are the power filling factors of double-clad fiber for pumping light and fiber laser, respectively. σ_{ap} and σ_{ep} are the absorption cross-section and emission cross-section of pumped light, respectively, σ_{as} and σ_{es} are the absorption cross-section and emission cross-section of laser, h is Planck constant, v_s and v_p are the frequency of laser and pumped light, respectively. τ is the average lifetime of the upper energy level of a particle, where $P_0 = 2hv_s\Delta v_s$ is the contribution of spontaneous radiation to the laser within the gain bandwidth, and its value is relatively small. This can be ignored later in the derivation, where Δv_s is gain bandwidth. Under steady-state conditions, the boundary conditions of the linear resonator laser are as follows:

$$\begin{cases} P_p^+(0) = P_p^l \\ P_p^-(L) = P_p^r \\ P_s^+(0) = R_1 P_s^-(0) \\ P_s^+(0) = R_2 P_s^+(L) \end{cases} \tag{34.2}$$

where P_p^l and P_p^r inject the pumping optical power of the inner cladding of the double-clad fiber from the left and right end faces, respectively. Therefore, the output power

of the fiber laser is

$$P_{out} = \frac{(1-R_2)\sqrt{R_1}.P_{s,sat}}{(1-R_1)\sqrt{R_2}+(1-R_2)\sqrt{R_1}}.\left[\frac{v_s}{v_p}.(1-\exp(-\Psi))\cdot\frac{P_p^+(0)+P_p^-(L)}{P_{s,sat}}\right.$$
$$\left.-(N\Gamma_s\sigma_{as}+a_s)L-\ln\left(\frac{1}{\sqrt{R_1R_2}}\right)\right] \tag{34.3}$$

$P_{s,sat} = hv_sA_c/[\tau\Gamma_s(\sigma_{es}+\sigma_{as})]$ is the output power of the saturated laser and $P_{p,sat} = hv_pA_c/[\tau\Gamma_p(\sigma_{ep}+\sigma_{ap})]$ is the pumping power of the saturated laser.

34.2.3 Numerical Simulation of a Double-Clad Fiber Laser

In view of the above analysis process, this section mainly introduces the results of numerical simulation. The doped fiber selected in this paper is Yb^{3+} particles, because the energy-level structure of Yb^{3+} is simple, and only two multistate expanded energy levels $^2F_{5/2}$ and $^2F_{7/2}$ are related to the wavelength of all light. For Yb^{3+}-doped fiber laser, the central wavelength of pumped LD is generally 915 nm or 975 nm, and the absorption cross-section of 975 nm is about three times that of 915 nm. The quantum efficiency of the laser is also relatively high, so 975 nm LD is used as the pumping source. The basic parameters of the double-clad fiber laser used in the above analysis and simulation are shown in Table 34.1.

Table 34.1 Basic parameters of fiber laser

Symbol	Physical parameters	Numerical value	Unit
λ_p	Pump light center wavelength	975	nm
λ_s	The central wavelength of a fiber laser	1064	nm
τ	Yb^{3+} upper energy level life of a particle	0.8	ms
σ_{ap}	The absorption cross-section of pumped light	2.6×10^{-20}	cm^2
σ_{ep}	The emission cross-section of pumped light	2.6×10^{-20}	cm^2
σ_{as}	The absorption cross-section of a fiber laser	1×10^{-23}	cm^2
σ_{es}	Emission cross-section of optical fiber laser	1.6×10^{-21}	cm^2
A_c	The cross-sectional area of the fiber core	3.1416×10^{-6}	cm^2
a_p	The loss of fiber to the pumped light	2×10^{-5}	cm^{-1}
a_s	Loss of optical fiber to the laser	4×10^{-5}	cm^{-1}
L	Length of optical fiber	20	m
Γ_p	Fill factor for pumping light	0.0024	No unit
Γ_s	Laser power filling factor	0.82	No unit
R_1	The reflectivity of the anterior cavity mirror	0.99	No unit
R_2	Reflectivity of the posterior cavity mirror	0.04	No unit

Pump power under different pumping modes

This section mainly introduces the experimental simulation results under different pumping modes, which simulate the output power of the laser resonator system in three directions: forward pumping, backward pumping, and two-way pumping.

As can be seen from Fig. 34.2, the output power of the laser resonator is not significantly different under the three pumping modes. However, the laser heat dissipation performance will be affected to some extent due to the backward pumping and bidirectional pumping methods. Therefore, these two pumping methods are generally not considered. It can be seen from Fig. 34.2a that the output power of the optical resonator system will increase with the increase of the length of the gain fiber, but it does not increase all the time. The growth rate will become slower and slower with the increase of the gain fiber. When the length of the gain fiber reaches a certain degree, the output power of the laser resonator system reaches a basically stable state. However, when the length of the gain fiber is increased, the output power will decrease. The length of the gain fiber is called the optimal fiber length. As for the output power, the reason is that the excessively long gain fiber will make the pump

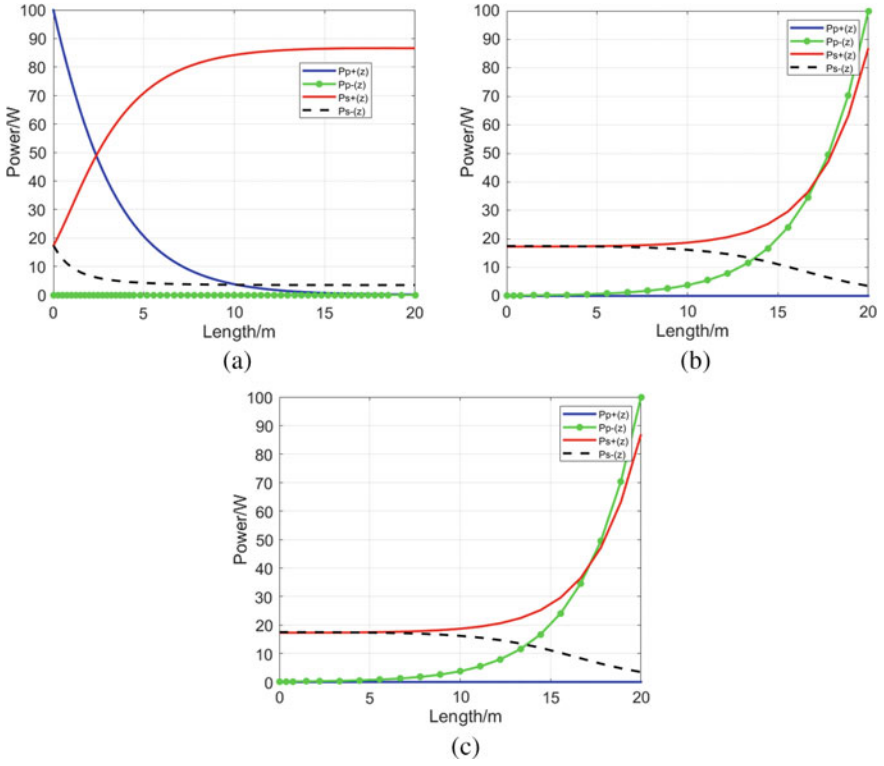

Fig. 34.2 The influence of different pumping modes on the output power of laser resonator system **a** forward pumping mode, **b** backward pumping mode, **c** two-way pumping mode

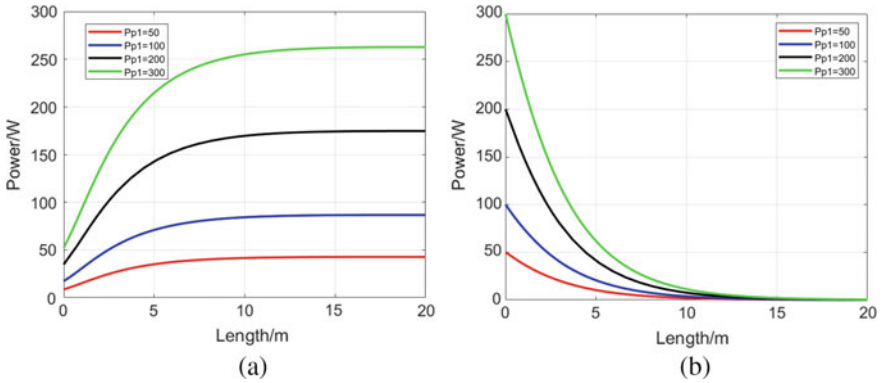

Fig. 34.3 Output power of **a** ytterbium-doped double-clad fiber laser with different pump power on fiber laser performance, **b** pump power

light source be completely absorbed before reaching the end of the fiber, and there is no inversion of particle number, but at this time, the signal light is still in very strong signal power so that the signal light is stimulated and absorbed, resulting in the decrease of the output power of the laser resonator system.

Effect of pump power on laser output

When the pumping power was 50, 100, 200, and 300 W, the doping concentration was 5.535×10^{19} cm^{-3}, and the fiber length was L = 20 m, the laser distribution in the fiber under the condition of forward pumping was simulated numerically. As can be seen from Fig. 34.3a, with the increase of the pump light power, the laser output power also increases. At the same time, the higher the pump power is, the longer the optimal gain fiber length is required to reach the stationary state. It can be seen from Fig. 34.3b that the higher the pump power is, the faster the attenuation rate of the pump is, and the longer the fiber length is required to reach the steady-state.

Influence of core doping concentration on output power

The doped concentration of the fiber core will affect the refractive index, which directly affects the amplification ability of the fiber. Therefore, under the premise that the pump power is 100 W and L = 20 m, change the doping concentration N to obtain the change curve of the output signal optical power and doping concentration. From Fig. 34.4a, it can be seen that the higher the doping concentration is, the faster the output power of the fiber laser grows, and the smaller the fiber length is required to obtain the maximum output power. At the same time, it is observed from Fig. 34.4b that the higher the doping concentration is, the faster the attenuation of the pump power is, and the shorter the transmission distance in the optical fiber is. The higher the doping concentration is, the higher the absorption degree of the fiber to the pump light is, so the maximum signal light output power can be achieved soon. In the remaining length of the fiber, the loss of the fiber will be accelerated, so the output power will be reduced.

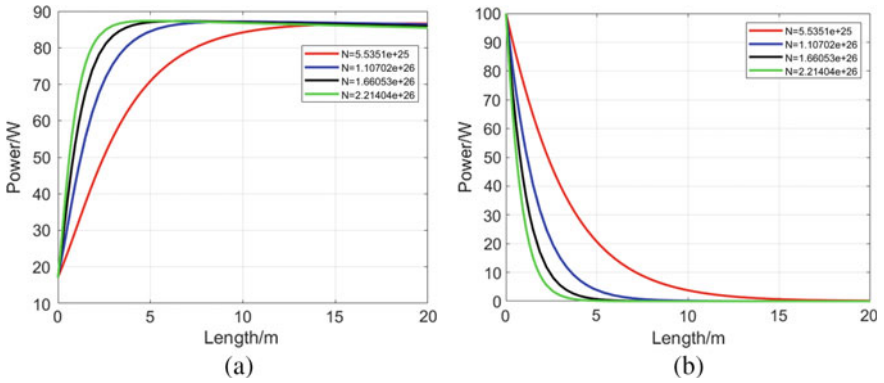

Fig. 34.4 Pump power changes of output power and pump power of ytterbium-doped double-clad fiber laser at different doping concentrations. **a** Output power of ytterbium-doped double-clad fiber laser. **b** Pump power

34.3 Experiment and Result Analysis of Fiber Laser

34.3.1 Experimental Setup

According to the basic structure composition of the double-clad fiber laser introduced in the previous section, it mainly includes pump source, fiber beam combiner, ytterbium-doped double-clad fiber, and fiber grating. So in order to get high power laser output, the pumping efficiency must be very high. The higher the pump power, the higher the output power of the laser. Therefore, the pump source is the diode-pumped laser (DPSSL). It can be seen from the previous Sect. 34.2.3 that forward pumping is the best under three kinds of pumping. The concentration of the doped fiber will affect the output power. Therefore, under the existing conditions, the gain fiber with the doping concentration of 4.0×10^{23} cm^{-3} is selected.

Based on the above analysis and the traditional gas detection system, a double-clad fiber laser gas detection system was built, as shown in Fig. 34.5. The emitted laser passes through a custom connector through KTP (frequency multiplexer) and becomes a central wavelength of 532 nm into a photonic crystal fiber. At the same time, the upper end of the T-interface is used to pass the gas into the photonic crystal optical fiber (HC-580-02, with 580 nm as the central wavelength) with high pressure so that the light interacts with the molecules of the sample to be measured and Raman scattering is generated. At the same time, the light waves without full effect continue to transmit in the photonic crystal fiber, and the FBG4 at one end of the fiber (with a reflectivity of 96% to 580 nm) is reflected back to FBG3 (with a reflectivity of 99% to 580 nm). It keeps oscillating in the optical resonator composed of FBG3 and FBG4, which increases the number of molecules involved in Raman scattering and improves the Raman intensity, finally through the photoelectric acquisition system, and then the data processing.

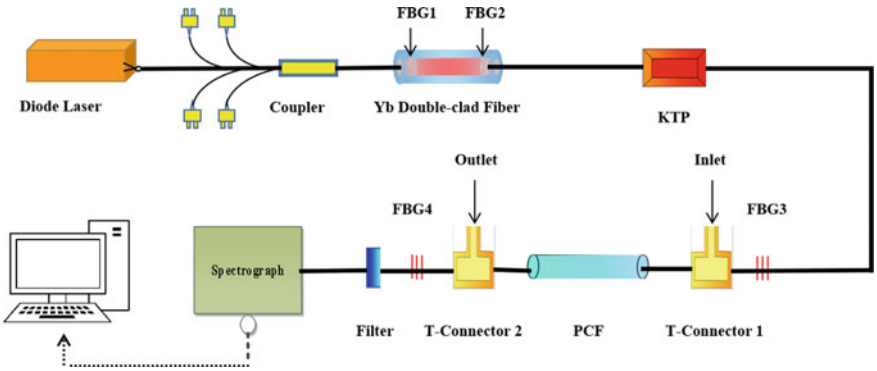

Fig. 34.5 The basic system of Raman gas detection for fiber laser

34.3.2 Test and Analysis of Experimental Equipment

Feasibility test of the experimental device

In optical detection, the laser diode is commonly used as the pump source. Therefore, the light source in Fig. 34.5 is replaced by the laser diode with an output power of 100 MW, forming a common optical detection system. In order to prevent the influence of the air in the optical path on the test results, nitrogen is first supplied for a period of time, and then 5% oxygen is aerated at 3 bar atmospheric pressure. As shown in Fig. 34.6a, it can be clearly seen that the oxygen Raman frequency shift occurs at 1556 cm^{-1}, which is consistent with the standard oxygen Raman frequency shift, proving that this optical detection system is feasible.

In order to explore the detection performance of the double-clad fiber laser as a light source, the above-mentioned laser diode was replaced with a double-clad laser

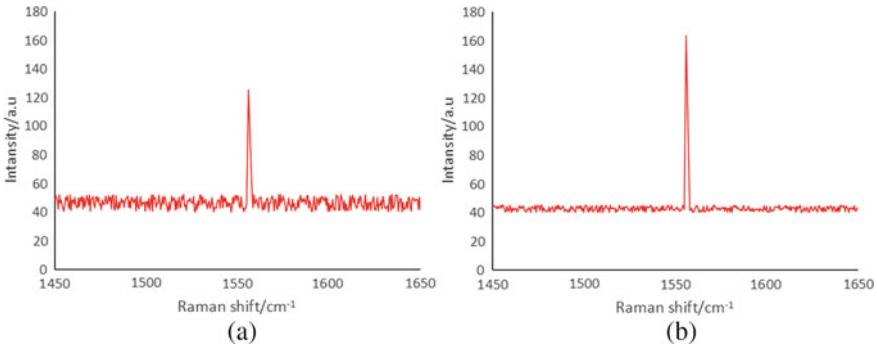

Fig. 34.6 Raman scattering diagram of oxygen molecules under different light sources. **a** Ordinary LD light source as detection light source **b** Ytterbium-doped double-clad fiber laser as detection light source

light source with an output power of 100 MW. As shown in Fig. 34.6b, it can also be seen that there is an oxygen Raman frequency shift at 1556 cm^{-1}, which indicates that neither the use of laser diode source as a Raman light source nor the double-clad fiber laser designed to detect the Raman light source will have any influence on the Raman frequency shift. But when laser diode and double-clad fiber laser are used as the Raman light source, the signal fluctuation is larger and the Raman intensity is smaller. Therefore, a double-clad fiber laser as a Raman detection source has better stability and sensitivity. Therefore, the linearity and stability of the experimental apparatus for the double-clad fiber laser as the light source are then tested.

Linearity test of the experimental device

Linearity is an important index of measuring the precision of a measuring instrument. In order to verify the sensitivity of the system, oxygen calibration experiments were carried out. Using EN4000 distribution device configuration range from 5 to 25% oxygen gas volume, respectively, to test the different concentrations of oxygen gas, oxygen concentration and intensity of Raman scattering is obtained by the experiment shown in Fig. 34.7a. The results of fitting, as shown in Fig. 34.7b, the result of oxygen concentration, and intensity of Raman scattering get an approximately linear relationship. The linear relationship between the two is $f(x) = 36.66591x - 1.85227$, and the linearity reaches 99.94%, indicating good linearity of the system.

Stability test of the experimental device

In order to verify the stability of the system, 10 portions of oxygen with concentrations of 5, 10, 15, 20 and 25% were configured for testing, and the experimental device was rinsed with nitrogen after each concentration of oxygen was tested to ensure the standard of oxygen concentration. The Raman test was carried out with oxygen at a concentration of 5% as an example, and the results were shown in the experimental test figure shown in Fig. 34.8a. The experimental results show that the oxygen concentration obtained from each experiment does not vary much. In the same

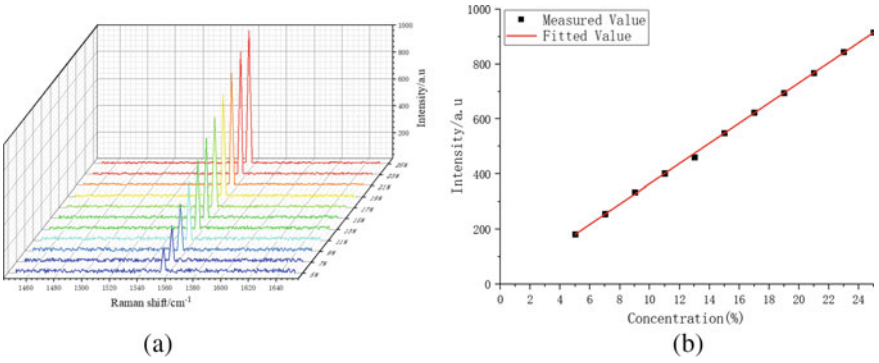

Fig. 34.7 Sensitivity test results of the experimental device. **a** Detection results under different gas concentrations. **b** Raman scattering intensity fitting of the gas under different concentrations

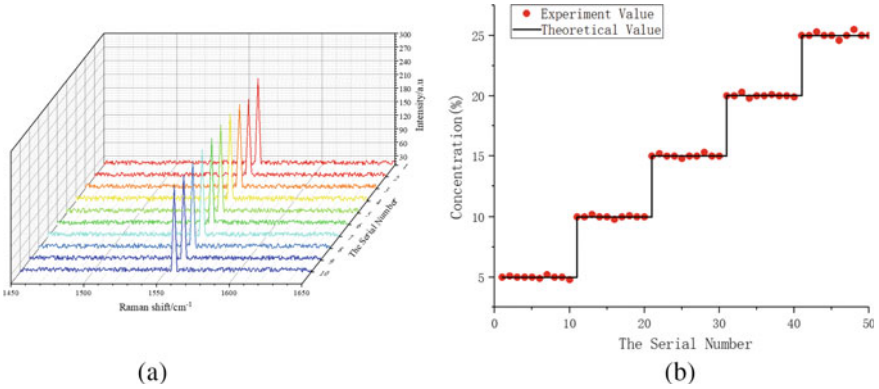

Fig. 34.8 Stability test results of the experimental setup. **a** Gas with 5% concentration measured multiple times Raman test diagram. **b** Gas repeatability test diagram at different concentrations

way, other oxygen concentrations were measured. In order to verify the stability of the experimental device, the obtained results are summarized to obtain the resulting figure as shown in Fig. 34.8b. The dot represents the measured results and the straight line represents the theoretical concentration. As can be seen from Fig. 34.8b, the experimental results are basically consistent with the standard concentration, and the average repetition rate is 99%, indicating good stability of the system.

34.4 Conclusions

It is found that the double-clad doped laser has good stability and high linearity as the detection light source. Moreover, when the output power of the double-clad laser is large, the scattering cross-section can be effectively changed to enhance the Raman effect and the detection accuracy of low-concentration materials can be improved. Part from the first part of the theoretical study shows different ways of pumping, fiber doping concentration, pump power on the performance of the double-clad fiber laser have influence, therefore can change the way double-clad fiber laser pumping, pump input power, doping concentration, etc. to increase the output power of double-clad fiber laser, in order to enhance Raman optical input power, enhance the Raman effect, and achieve the low concentration gas detection.

Acknowledgements The authors acknowledge the financial support of the National Key R&D program of China (2019YFB1705800), and the 15th Batch of Jiangsu province "six talent peaks" high-level talent project (GDZB-042)

References

1. C.J. Halcrow, C. King, N.S. Manton, Oxygen-16 spectrum from tetrahedral vibrations and their rotational excitations. Int. J. Mod. Phys. **28**(04), 1950026 (2019)
2. R. Salter, J. Chu, M. Hippler, Cavity-enhanced Raman spectroscopy with optical feedback cw diode lasers for gas phase analysis and spectroscopy. Analyst **137**(20), 4669–4676 (2012)
3. L. Zou, Y. Yao, J. Li, High-power, efficient and azimuthally polarized ytterbium-doped fiber laser. Opt. Lett. **40**(2), 229–232 (2015)
4. X. Liu, J. Chen, J. Han et al., Design of large mode area total internal reflection photonic crystal fiber for high power fiber laser. High Power Laser Part. Beams **26**(10), 71–76 (2014)
5. H. Tian, Z. Hou, S. Zhang, G. Zhou et al., Research on ytterbium-doped photonic crystal fiber amplifier for the femtosecond fiber laser. Laser Phys. **26**(1), 1–6 (2016)
6. N. Nishizawa, Development and application of fiber laser. Appl. Opt. **42**(2), 438–445 (2013)
7. D. Mgharaz, N. Rouchdi, A. Boulezhar et al., Double-clad fiber laser design for particle image velocimetry and material science applications. Opt. Lasers Eng. **49**(1), 1–7 (2011)